

High-Performance Carbon Dioxide Capture and Storage by Multi-Functional Sphingosine Kinase Inhibitors through a CO₂-philic Membrane

Seyede Tahereh Hosseini,^[a] Heidar Raissi,^[b] Majid Pakdel^{[c]*}

[a] S. T. Hosseini

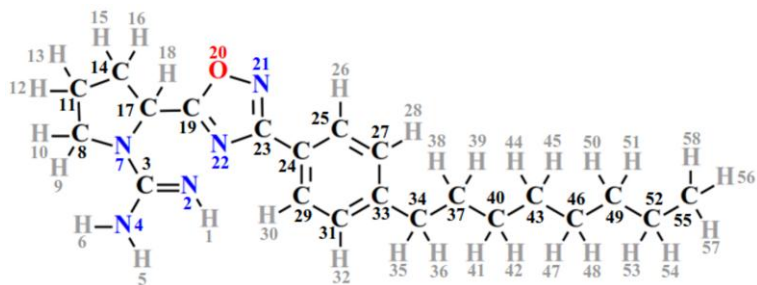
*Department of Chemistry, Faculty of Science, University of Birjand, Birjand, Iran
E-mail address: t.hosseyini.chemphy@birjand.ac.ir*

[b] H. Raissi

*Department of Chemistry, Faculty of Science, University of Birjand, Birjand, Iran
E-mail address: hraeisi@birjand.ac.ir*

[c] M. Pakdel*

*Department of Chemistry, Faculty of Science, University of Birjand, Birjand, Iran
E-mail address: M.pakdel.chemphy@birjand.ac.ir*



Scheme S1. The schematic structure of SphKI molecule with atom labeling; carbon, hydrogen, nitrogen and oxygen labeled by black, gray, blue and red colors, respectively.

Table S1. Atom type and LJ parameters for SphKI molecule.

Atom type	σ [nm]	ϵ [kJ/mol]
1	0.363487	0.209200
2	0.329632	0.836800
3	0.329632	0.836800
4	0.363487	0.209200
5	0.355005	0.292880
6	0.040001	0.192464
7	0.329632	0.836800
8	0.356359	0.460240
9	0.329632	0.836800
10	0.040001	0.192464
11	0.387541	0.230120
12	0.235197	0.092048
13	0.329632	0.836800

Table S2. Atom label, atom type and charges for SphKI molecule.

Atom number	Atom type	Charge [e]	Atom number	Atom type	Charge [e]
1	1	0.382	30	12	0.272
2	2	-0.897	31	12	-0.233
3	3	0.631	32	12	0.261
4	4	-0.921	33	12	-0.018
5	5	0.447	34	11	-0.499
6	5	0.440	35	12	0.265
7	5	-0.536	36	12	0.264
8	5	-0.270	37	11	-0.484
9	5	0.267	38	12	0.245
10	5	0.248	39	12	0.245
11	6	-0.497	40	11	-0.476
12	7	0.260	41	12	0.241
13	8	0.275	42	12	0.241
14	9	-0.476	43	11	-0.477
15	10	0.280	44	12	0.240
16	10	0.265	45	12	0.240
17	9	-0.123	46	11	-0.478
18	11	0.284	47	12	0.239
19	12	0.594	48	12	0.239
20	12	-0.336	49	11	-0.479
21	11	-0.182	50	12	0.238
22	12	-0.535	51	12	0.238
23	12	0.344	52	11	-0.489
24	11	-0.122	53	12	0.240
25	12	-0.198	54	12	0.240
26	12	0.269	55	11	-0.710
27	11	-0.260	56	12	0.239
28	12	0.262	57	12	0.246
29	13	-0.222	58	12	0.239

Table S3. LJ parameters and charges for CO₂ molecule.

	C atom	O atom
q (e)	0.6512	-0.3256
ϵ (kJ/mol)	0.2340	0.6683
σ (nm)	0.2800	0.3028

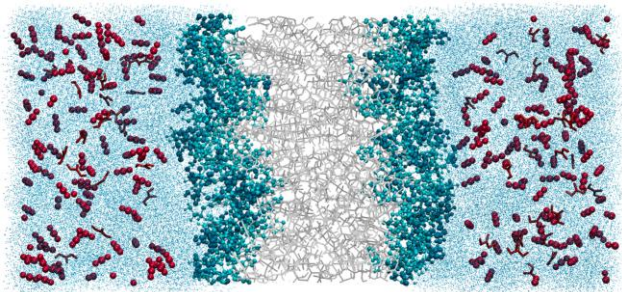


Figure S1. The initial simulation box (before a simulation run) for CO₂-SphKI system. CO₂, H₂CO₃ and water molecules are colored in light red (CPK format), dark red (licorice format) and cyan (point format), respectively. Ions are left invisible.

Local Nucleophilicity

The electrophilic (P_k^+) and nucleophilic (P_k^-) Parr functions of a molecule can be described by conceptual density functional theory, which are given by the following equations:

$$P^-(r) = \rho_s^{rc}(r) \quad \text{for electrophilic attacks} \quad (1)$$

$$P^+(r) = \rho_s^{ra}(r) \quad \text{for nucleophilic attacks} \quad (2)$$

where $\rho_s^{rc}(r)$ is the atomic spin density at the “r” atom of the radical cation (charge = +1; multiplicity = 2) and $\rho_s^{ra}(r)$ is the atomic spin density at the “r” atom of the radical anion (charge = -1; multiplicity = 2). With the optimized neutral molecular structure at hand, each atomic spin density gathered at the different atoms of the radical cation (rc) and the radical anion (ra), which provides the local electrophilic and nucleophilic Parr functions of the neutral molecule. In this study, nucleophilic (P_k^-) Parr function was obtained at the UM06-2X/6-31+G** computational level (single point energy).

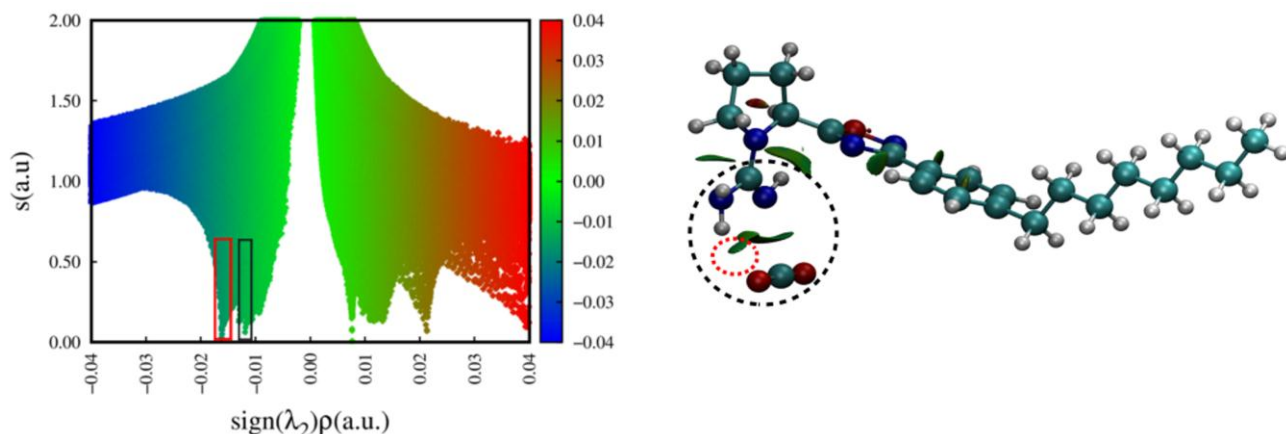


Figure S2. (left) M06-2X/6-31+G** 2D plot of RDG, $s(r)$, versus $\text{sign}(\lambda_2)\rho(r)$ for complex 1 (C1). (right) NCI 3D isosurfaces of C1 generated by NCIPLOT 3.0 program and visualized by VMD 1.9.

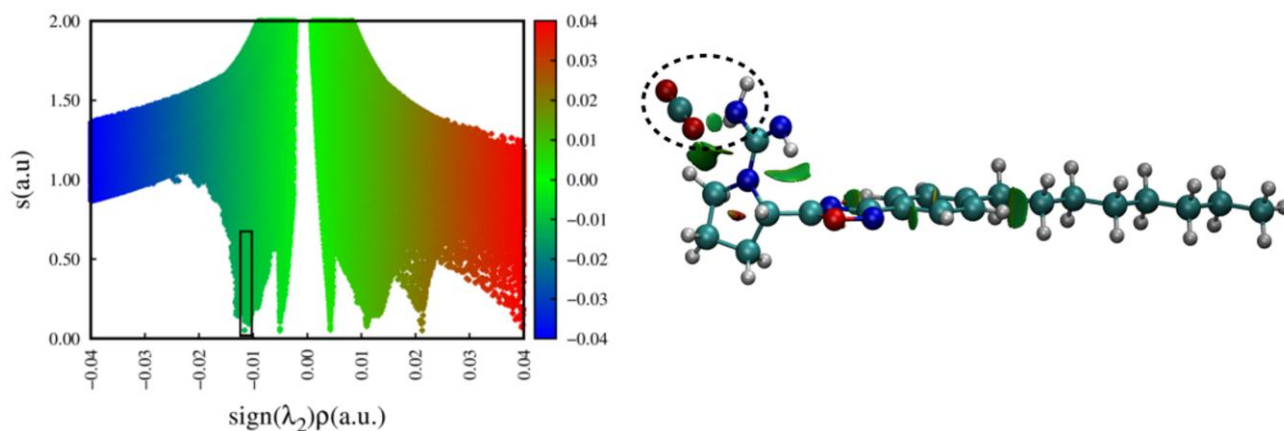


Figure S3. (left) M06-2X/6-31+G** 2D plot of RDG, $s(r)$, versus $\text{sign}(\lambda_2)\rho(r)$ for complex 2 (C2). (right) NCI 3D isosurfaces of C2 generated by NCIPLOT 3.0 program and visualized by VMD 1.9.

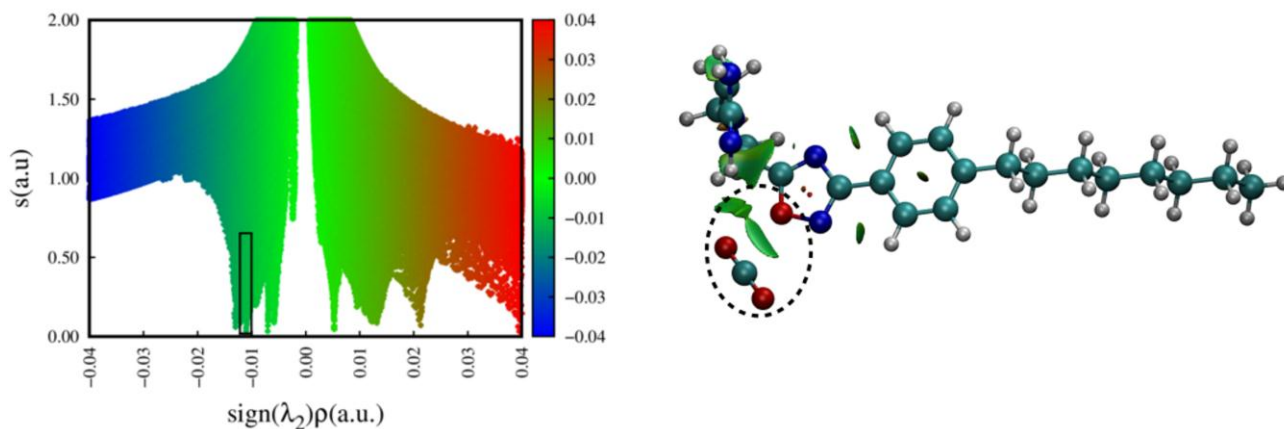


Figure S4. (left) M06-2X/6-31+G** 2D plot of RDG, $s(r)$, versus $\text{sign}(\lambda_2)\rho(r)$ for complex 5 (C5). (right) NCI 3D isosurfaces of C5 generated by NCIPLOT 3.0 program and visualized by VMD 1.9.

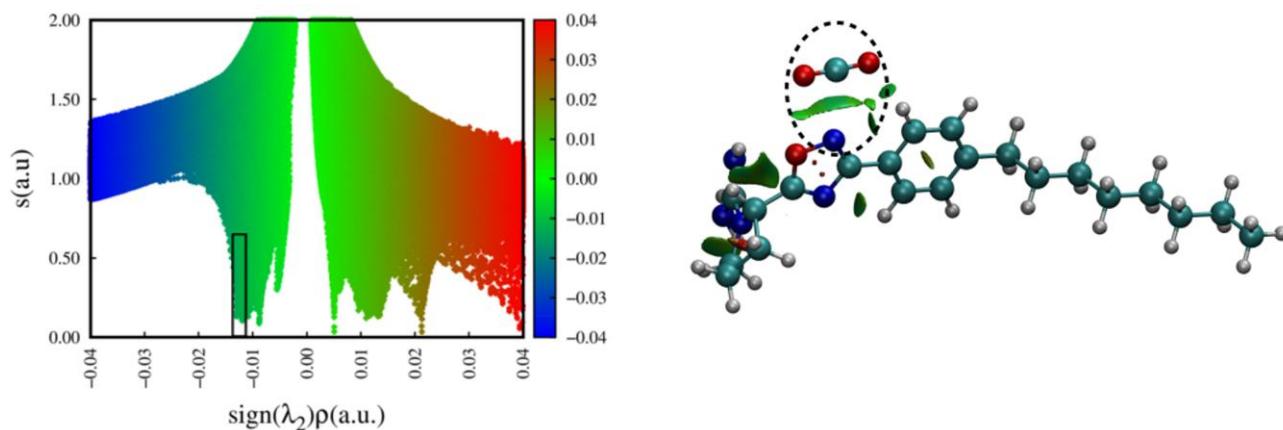


Figure S5. (left) M06-2X/6-31+G** 2D plot of RDG, $s(r)$, versus $\text{sign}(\lambda_2)\rho(r)$ for complex 6 (C6). (right) NCI 3D isosurfaces of C6 generated by NCIPLOT 3.0 program and visualized by VMD 1.9.

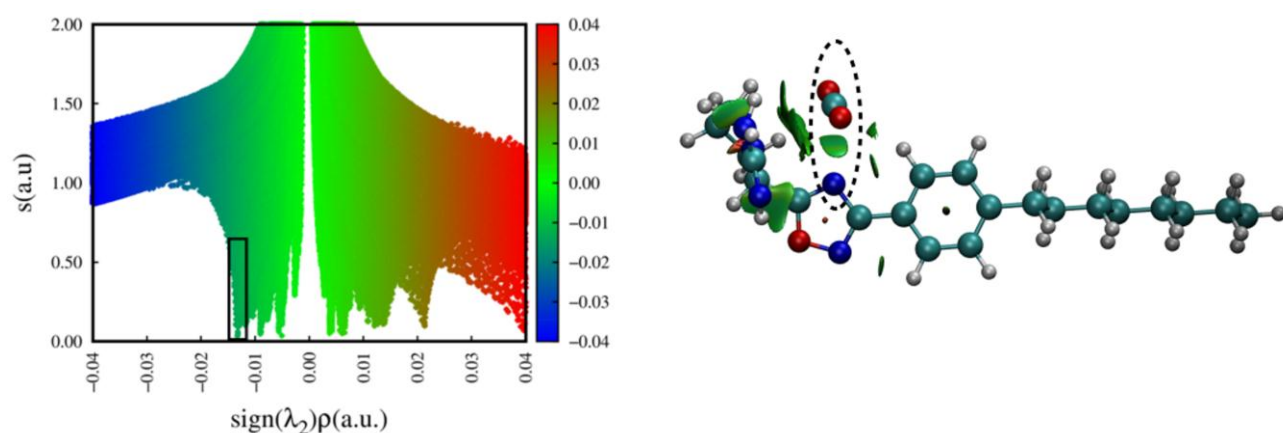


Figure S6. (left) M06-2X/6-31+G** 2D plot of RDG, $s(r)$, versus $\text{sign}(\lambda_2)\rho(r)$ for complex 7 (C7). (right) NCI 3D isosurfaces of C7 generated by NCIPLOT 3.0 program and visualized by VMD 1.9.

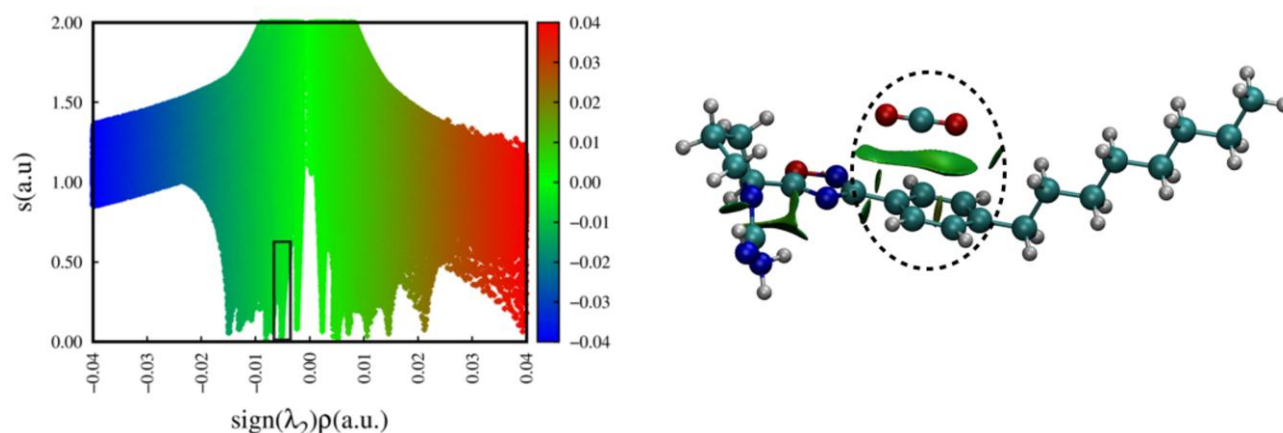


Figure S7. (left) M06-2X/6-31+G** 2D plot of RDG, $s(r)$, versus $\text{sign}(\lambda_2)\rho(r)$ for complex 8 (C8). (right) NCI 3D isosurfaces of C8 generated by NCIPLOT 3.0 program and visualized by VMD 1.9.

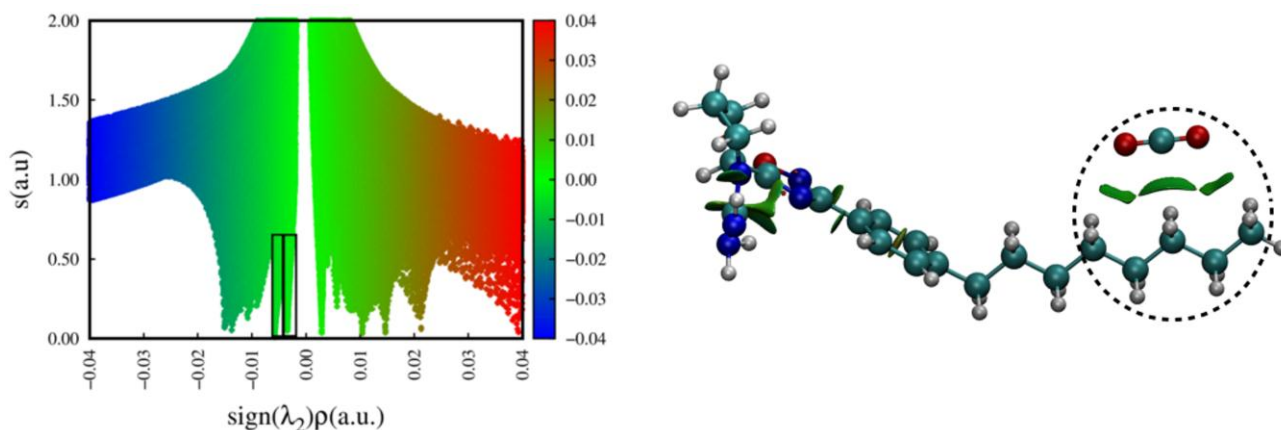


Figure S8. (left) M06-2X/6-31+G** 2D plot of RDG, $s(r)$, versus $\text{sign}(\lambda_2)\rho(r)$ for complex 9 (C9). (right) NCI 3D isosurfaces of C9 generated by NCIPLOT 3.0 program and visualized by VMD 1.9.

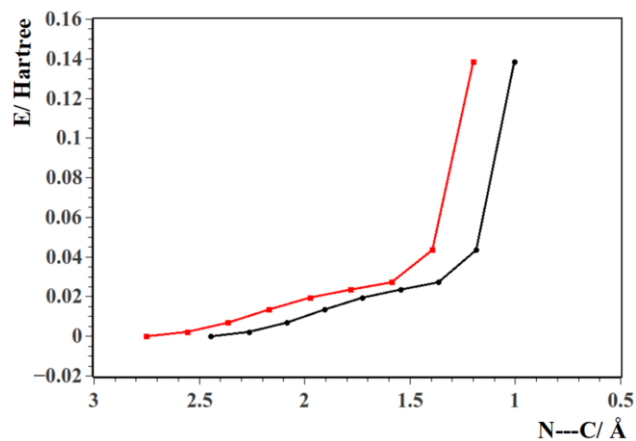


Figure S9. The two potential energy surface scan (PES) curves of $\text{N2-C}(\text{CO}_2)$ (black) and $\text{N3-C}(\text{CO}_2)$ (red) obtained by DFT calculations.

Table S4. Thermodynamic data, in Hartree (including unique imaginary frequency of TS, in cm^{-1}) of the located stationary points in the SphKI(N1)- CO_2 reaction at 25°C .

Stationary points	Sum of electronic and zero-point correction energies (Hartree)	Thermal correction to Gibbs free energy (Hartree)	Imaginary frequency (cm^{-1})
SphKI + CO_2	-1355.456854	0.448457	-
TS	-1355.452631	0.450518	-263.1
SphKI- CO_2	-1355.473419	0.454373	-